WILEY-VCH

On the Reproductive Mechanism of Multilamellar Protocells

Dheeraj Kanaparthi[1&2*], Marko Lampe[4], Jan-Hagen Krohn[1], Baoli Zhu[2&4], Andreas Klingl[5], & Tillmann Lueders[2*]

[1]Max-Planck Institute for Biochemistry, Munich, Germany.
[2]Chair of Ecological Microbiology, BayCeer, University of Bayreuth, Germany.
[3]Advanced Light Microscopy Facility, European Molecular Biology Laboratory, Heidelberg, Germany.
[4]Key Laboratory of Agro-ecological Processes in Subtropical Regions,
CAS, Changsha, China.
[5]Department of Biology, LMU, Planegg-Martinsried, Germany.

*Corresponding authors

WILEY-VCH

Abstract: Bottom-up synthetic biology attempts to reconstitute the emergence of life through building a minimal self-reproducing cell. In spite of exciting recent breakthroughs, achieving reproduction independent of cell replication machinery still a daunting task. To achieve reproduction independent of canonical molecular biological processes, here we worked with bacterial protoplasts under environmental conditions of early Earth. Rather than reproducing in a chaotic manner due to the loss of molecular biological co-ordination, protoplasts in our study reproduced in a defined sequence of steps. Lifecycle of these protoplasts resemble vesicles undergoing osmotic shrinkage or expansion under flow. Morphological transformation and fission of parent cell into multiple daughter cells can be explained by an interplay between intracellular metabolism, physicochemical properties of cell constituents and environmental conditions. In short, our study demonstrates how cells reproduced prior to the evolution of molecular biological processes.

Introduction

Life on Earth is thought to have emerged in a series of steps described by the theory of chemical evolution[1]. According to this theory, organic compounds required for building a cell were synthesized by Miller-Urey[2]-like processes and subsequent prebiotic chemical reactions[3–5]. Eventually, these organic compounds coalesced to form a protocell[6,7]. These protocells were thought to have been very primitive and can essentially be described as lipid vesicles with internal chemical reactions. Unlike the present-day cells, whose morphology, growth, and reproductive processes are tightly controlled by molecular biological processes, such processes in protocells are thought to have been determined by the physical and chemical properties of their constituents[7,8]. Despite being a key evolutionary link between prebiotic chemical reactions and prokaryotes, protocells to date remained a theoretical possibility with no definitive proof for their existence on early Earth, nor was it demonstrated that physical and chemical properties of cell constituents alone could mediate complex biological processes like cell replication. In the present study, we attempted to achieve cell fission leading to the formation of metabolically viable daughter cells, independent of molecular biological processes and mediated entirely by physicochemical properties of cell constituents.

Our study differs from earlier studies on protocells in two key aspects. First, rather than the conventional choice of using lipid vesicles (LVs), here we used protoplasts of the Gram-negative bacterium *Rhodobacter sphaeroides* (*RS-P*) as a proxy protocell. In our opinion, bacterial protoplasts better simulate a primitive protocell than lipid vesicles for several reasons. Unlike the LVs that must be constantly fed with micelles to induce growth and subsequent reproduction[7], protoplasts possess an internal metabolism and are capable of self-sustained growth. Protoplasts are physiologically and chemically more complex than LVs. In our opinion, even the most primitive self-replicating protocells should have possessed an internal metabolism and should have been more complex in their chemical composition than typical LVs. Nevertheless, protoplasts like the protocells, lack the innate ability to regulate either their morphology or reproduction[9,10]. Hence, we consider bacterial protoplasts to be better proxies for studying protocell reproduction than LVs[11]. As the second novelty of our study, we grew these protoplasts under prebiotically plausible environmental conditions.

The exact environmental conditions of early Earth are a matter of debate among researchers; Nevertheless, recent consensus among researchers suggests that surface temperatures of Archaean Earth

WILEY-VCH

(4000-2500 million years ago) ranged between 26° to 35°C[13,14] and Archaean Eon ocean were 1.5 to 2 times saltier than the current oceans[15]. To replicate these conditions, we grew *RS-P* in half-strength nutrient broth (NB) supplemented with 5-10% Dead Sea salt (DSS) at 30°C. DSS was used in our incubations rather than pure NaCl to replicate the complex salt composition of Archaean oceans[16,17]. Ones we obtained stable protoplasts of *Rhodobacter sphaeroides* (*RS-P*), we transferred them into fresh growth media and monitored their morphological transformation at regular intervals (methods section). In the below sections of the manuscript, we present an in-depth morphological transformation of *RS-P*, together with an explanation of the physicochemical mechanisms driving such transformations.

Results and Discussion

Morphological transformation of *RS-P* was monitored at regular intervals by staining and observing the cells using a wide array of Super-resolution microscopic techniques. A simplistic version of *RS-P*'s lifecycle is presented in Figure 1.

During the lag phase, growth was restricted to the outer membrane of the cell, which expanded to form a hollow filamentous extension (Figure 1b, c & S1). The length of this tail varied from cell to cell, ranging between 0.5 to 5 µm (Figure 1b, 1c & Figure S1a). Based on our observations we propose a

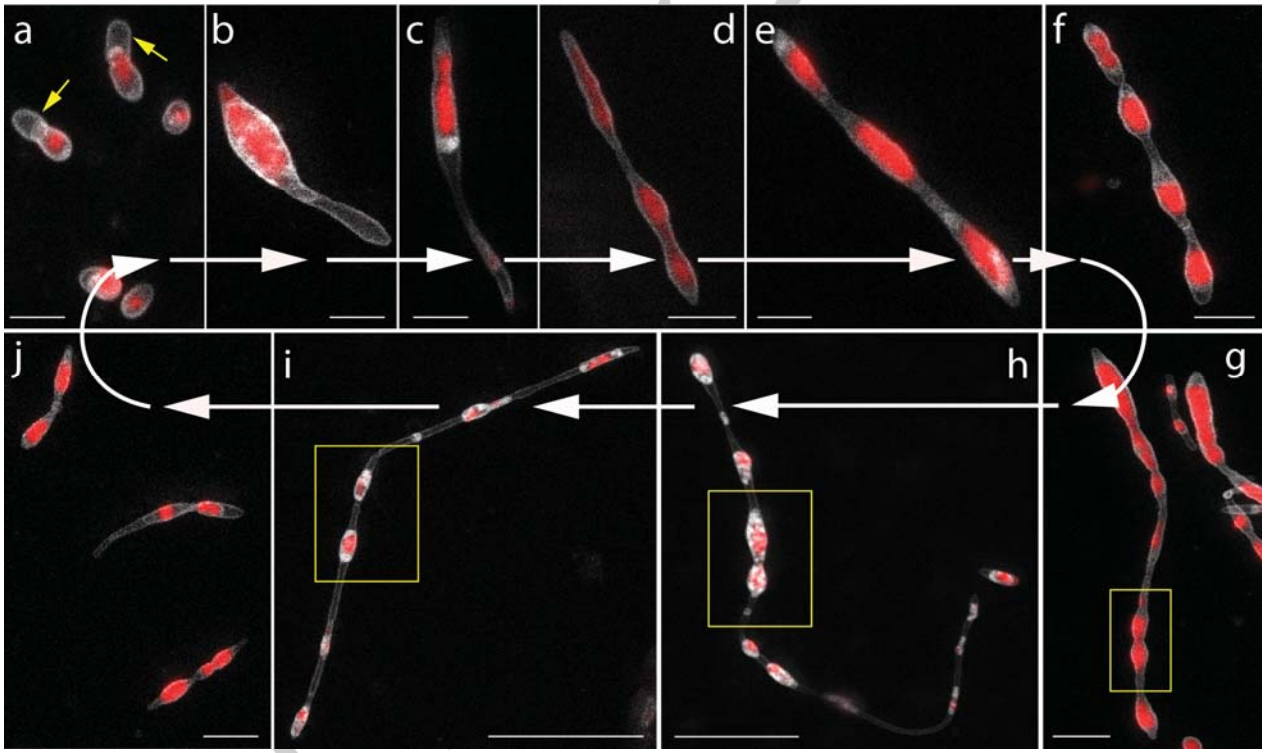

***Figure 1*. Lifecycle of *RS-P*.** Images a-j, show the sequential morphological transformation of *RS-P*. Images were acquired using a STED microscope and cells in these images were stained with universal membrane stain, FM™5-95 (white), and DNA stain, PicoGreen™ (red). Arrows within the image point to the cyclic transformation of *RS-P*. Yellow arrows in image-a show cells with outer membrane extensions (also in b, c & Figure S1). Boxes in images g-i show cytoplasmic compartments within the filamentous cell undergoing binary fission. Image j shows individual cells with membrane overhangs formed from the fragmentation of filamentous cells. Subsequent transfer of these cells into fresh media

results in repetition of this process, suggesting that daughter cells formed are metabolically viable. Scale bars: 2µm (a-g & j) and 10µm (h & i).

two-step process by which the hollow membrane extensions were formed. In the first step, disproportionately high lipid synthesis in comparison to cytoplasmic volume increase (low growth rate during lag-phase) in *RS-P* should have facilitated the transformation of the excess membrane into a bud (Figure S1e). This phenomenon of excessive lipid synthesis in bacterial protoplasts was reported by earlier studies[18]. Subsequently, these hollow buds detached from the inner membrane and were released into the space between outer and inner membranes (periplasmic space). Transmission electron microscope (TEM) images of this growth stage *RS-P*, show the presence of such buds in the periplasmic space (Figure S1e). In step two, these hollow vesicles fused and incorporated into the outer membrane, leading to its expansion and formation of a hollow filamentous structure (Figure 1b & Figure S1 a, b, e-g).

During the early-log phase, with an increase in the growth rate (Figure 2), the volume of the cytoplasm increased, gradually filling in the hollow template created by the outer membrane (Figure 1c & d). Phase-contrast and TEM images of such cells was shown in Figure S1. This led to the transformation of cells in sequence from spherical to tubular cells (Figure 1&2) and then into filamentous cells with cytoplasm mostly restricted to either end of the cell, resembling dumbbells with long filamentous connections (Figure 2, early log-phase). In the subsequent growth stages, cells developed surface depressions along their length resembling tubular vesicles subjected to curvature-induced destabilization at their surface (resembling Rayleigh-Plateau instability) (Figure 1d-g, Figure 2-late log phase & S2). These surface depressions were formed as a result of cytoplasmic compartment surrounded by the inner membrane undergoing binary fission (Figure 1 d-h). In some filamentous cells, we observed cytoplasmic compartments undergoing symmetric division leading to the formation of daughter cells

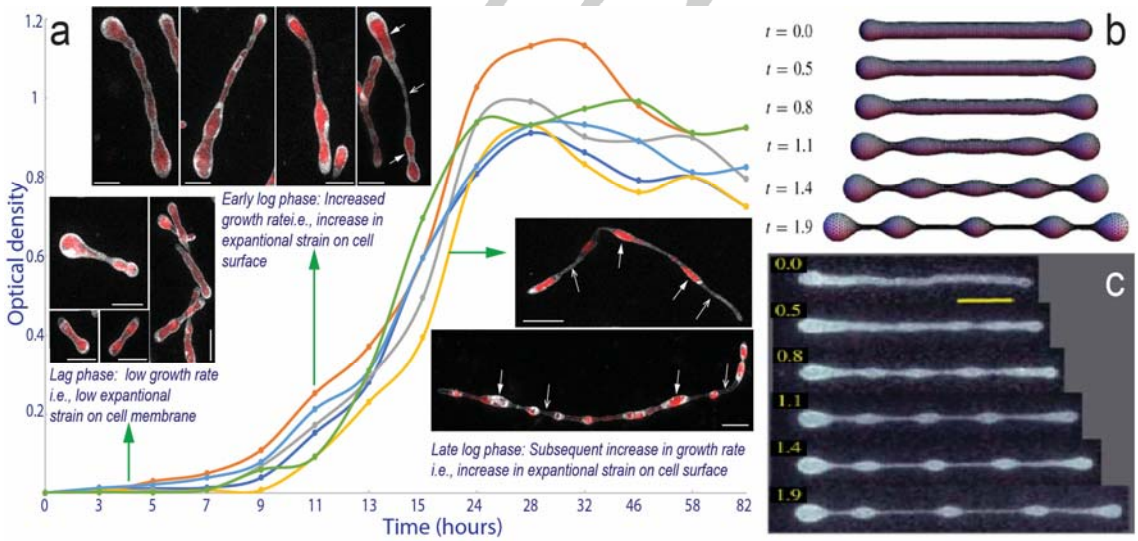

***Figure 2*. Comparison of *RS-P*'s morphology with theoretical predictions.** Image-a show growth curve and morphologies of *RS-P* in different growth stages. Cells were stained, imaged, and color-coded as described in Figure. 1. Closed and open arrows in the image point to regions of the cell with cytoplasm and hollow outer membrane connecting the cytoplasmic compartments respectively (also shown in Figure 4 & S2). Images b & c show theoretically predicted, and experimentally observed

morphologies of vesicles subjected to elongational stress over time (t) (originally published by Narsimhan et al., 2015[19], reproduced here with permission from Cambridge University Press). Scale bar: 1μm (lag & early log-phase), 10μm (late log-phase).

of equal sizes (Figure 1e & f). In such cells, surface depressions are uniform in size and regularly spaced. Alternately, some cells developed unevenly sized depressions with a large lenticular structure either at the tip (Figure 3, S1b-d & S3) or center of the filament (Figure 3 & S3). Such structures were formed due to asymmetric division of cytoplasmic compartments. Over time these surface depressions grew deeper and two adjacent cytoplasmic compartments were linked to each other only by a hollow strand of outer membrane (boxed regions in Figure 1h, 1i & Figure 2 – late log phase). Rupture of the outer membrane connections led to the formation of individual daughter cells (Figure 1j). Transformation of cells from spherical into a string of beads morphology, in this exact sequence, was reported earlier in LV's undergoing expansion in a laminar flow path[9,20] (Figure 2b, 2c & S2) and undergoing osmotic shrinkage[20,21]. Like the LVs, the above presented morphological transformation of *RS-P* can be explained by an interplay between intracellular metabolism, and physicochemical properties of cell constituents.

Growth (or expansion) of the cytoplasmic compartment of *RS-P*, gradually filling the void left by the outer membrane resembles a vesicle undergoing stretching when placed in an elongational flow path (Figure 2 & S2). Morphological transformation of vesicles undergoing such stretching is dependent on physicochemical properties of their membrane-like their elasticity and expansion strain[19,22]. Vesicles experiencing a low elongational strain are shown to transform into prolate or tubular shapes[22] (Figure 2b&c). However, at a certain strain level (threshold strain), vesicles transformed into a dumbbell morphology. Upon further strain increase, vesicles formed elongated dumbbells with beaded structures appearing along its length. *RS-P* exhibited a similar pattern of morphological transformation (Figure 2 & S2). In the case of *RS-P*, high and low elongational strains on the membrane translate into high and low growth rates. In accordance with our presumption, short prolate or tubular cells were most frequently observed during an early lag phase, when the growth rate of the cell was slower compared to other stages (Figure 2). With an increase in their growth rate, *RS-P* transformed into a dumbbell shape (Figure 2). During the mid/late-log phase, they formed elongated dumbbells with beaded structures along their length (Figure 2). The subsequent reduction in the growth rate during the stationary phase, transformed *RS-P* into string-of-beads morphology (Figure 1h & I, 2 and S2). Continuous transfer of log-phase cells every few hours into fresh media resulted in thicker and longer tubular *RS-P* cells (Figure S4). Unlike the cells in our batch incubations, these cells did not develop surface deformations. These results suggest that the rate of cytoplasmic volume increase (i.e., growth rate) of *RS-P* played an important role in determining its morphology.

Along with the growth rate, the morphological transformation of *RS-P* can also be explained from a physicochemical perspective. The lifecycle observed in *RS-P* is similar to LVs undergoing osmotic deflation[23]. This sequence of morphological transformations and the end morphology of such vesicles can be explained by Area differential elasticity (ADE) theory[20,21] and is largely determined by the physical properties of the membrane-like its elasticity, cell volume, and the amount of excess membrane. It was experimentally demonstrated that vesicles undergoing osmotic deflation, transform in sequence from spherical to prolate, tubular, then to tubular cells with surface depressions, and finally into a string-of-beads morphology to attain a thermodynamically lower energy state[20]. *RS-P* exhibited a very similar sequence of morphological transformation (Figure 1&2). Like the LVs, excessive lipid synthesis in protoplasts[18] keeps *RS-P* in a state of non-equilibrium between the surface area of the cell membrane and cytoplasmic volume. During the lag phase, this state of non-equilibrium could have

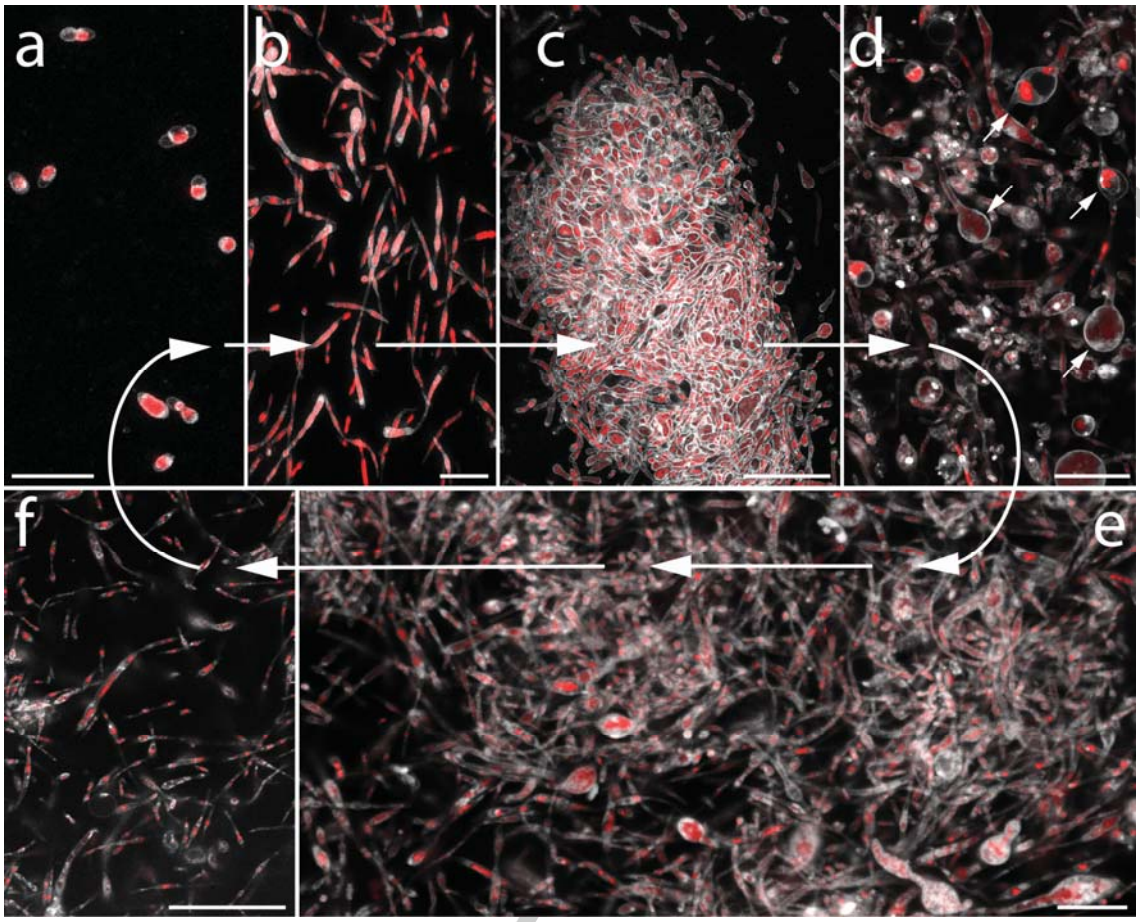

***Figure 3*. community images of *RS-P* at different growth stages**. Images a-f show morphological transformation of *RS-P* cells at different growth stages. Cells were stained, imaged and color coded as described in Figure. 1. Scale bars: 10μm.

caused *RS-P* to form hollow membrane extensions to accommodate this excess membrane. During the early and mid-log phases, the rate of cytoplasmic volume increase keeps pace with membrane synthesis. Hence, cells in this growth stage do not develop hollow membrane extensions (Figure 4c-j). A gradual decrease in the growth rate by the end of log-phase due to the depletion of nutrients in growth media, caused cells to revert to a state of membrane excess. This high ratio of the cell membrane to cytoplasmic volume led cells to transform into a string-of-beads morphology (Figure 1&2). Despite providing a mechanistic explanation for the morphologies of *RS-P*, neither vesicles undergoing expansion in a laminar flow path[9,20] nor LVs undergoing osmotic shrinkage[20,21], were ever reported to have formed large lenticular cells (Figures 3 & S3).

Formation of large lenticular or spheroid structures (Figure 3) with filamentous extensions could be explained by anisotropy in physical properties of cell membrane[24] (Figure 4). Biophysical studies focused on understanding morphology and cell replication have mostly been performed on LVs of simpler lipid composition. In such studies, it is generally assumed that the physical properties of the vesicle membrane like fluidity and elasticity are isotropic throughout their surface. Unlike LVs, cell membranes have a complex lipid composition and are intercalated with proteins. This leads to lateral heterogeneity or anisotropy in their physical properties[25]. It was hypothesized that such differences could result in a non-uniform expansion and deformation of membrane surface during osmotic

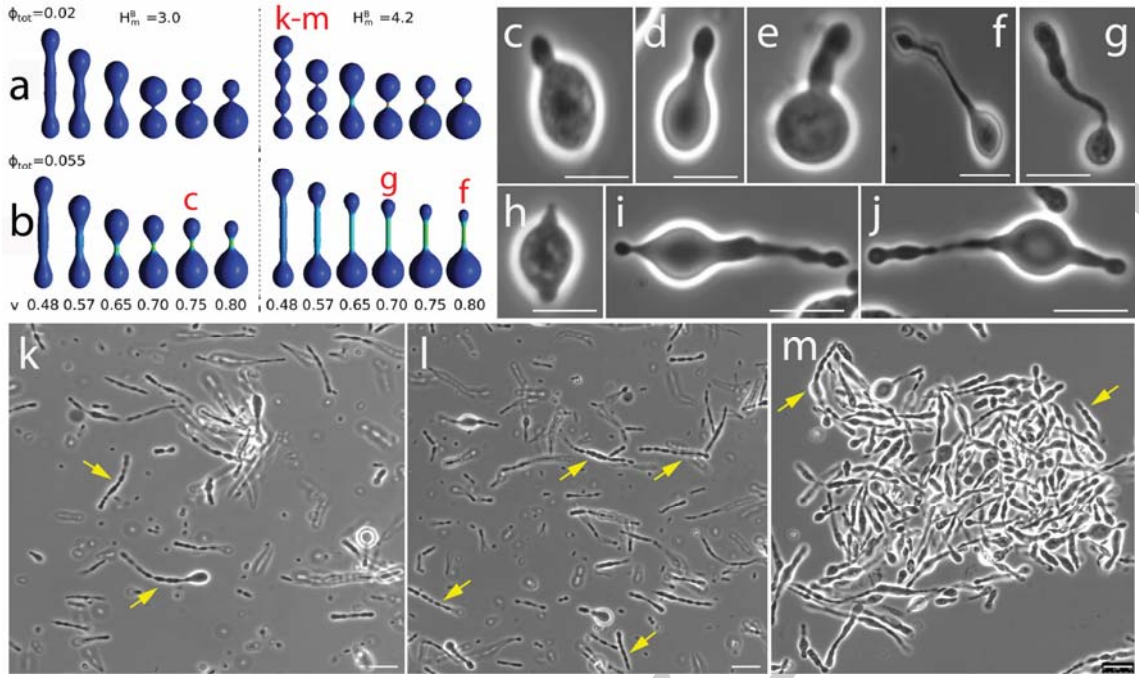

Figure 4. Comparison of *RS-P*'s morphology with theoretical predictions. Images a & b show morphologies of vesicles with an anisotropic membrane as predicted from mathematical models[24]. v-values (X-axis) represent the ratio between the actual volume of the vesicle to the volume of the same vesicle in its spherical form with the same surface area, Φ_{tot} – represents the concentration of an anisotropic component, $H^B{}_m$ – represents intrinsic curvature of the anisotropic component (originally published by Bobrovska *et al*., 2013)[24]. Images c-j, show lag and early log phase cells, that were very similar to the mathematically predicted morphologies (indicated by letters in red over the predicted shapes in image b). Images k-m show late-log phase *RS-P* cells, beginning to transform into a string-of-beads morphology (arrows). Scale bars: 2µm (c-j) and 10µm (k-m).

deflation, leading to an asymmetric cell division and possibly to the formation of lenticular structures[23] (Figure 4a & 4b). As shown in Figure 4b, the formation of thin tubular protrusions from a spherical cell could be a result of anisotropic nature of cell membranes[24]. The morphological transformation we observed in *RS-P* are very similar to the theoretical predictions on the behavior of LVs with anisotropic membranes (Figure 4). A high rate of cytoplasmic volume increase during the early (log-)growth stages represents a cell state with a higher value of v (reduced volume i.e., the ratio of actual vesicle volume and volume of the vesicle in spherical form) and high Φ_{tot} (inherently high lateral heterogenicity in live cells) *i.e.*, a state of little to no excess membrane. As predicted by the mathematical models, cells in this growth stage underwent an asymmetric division (Figure 4b-d) and the formation of filamentous protrusions. Figure S1f&g shows TEM images of *RS-P* cells forming such filamentous protrusions. Such asymmetric division of cytoplasmic content could have led to the formation of daughter cells of unequal sizes[24] in *RS-P*. A gradual reduction in the growth rate towards the end of the log phase could have resulted in lower v-values in *RS-P*. This reduction in v-values together with an increase in the spontaneous curvature due to excess membrane could have transformed *RS-P* into a string-of-beads morphology.

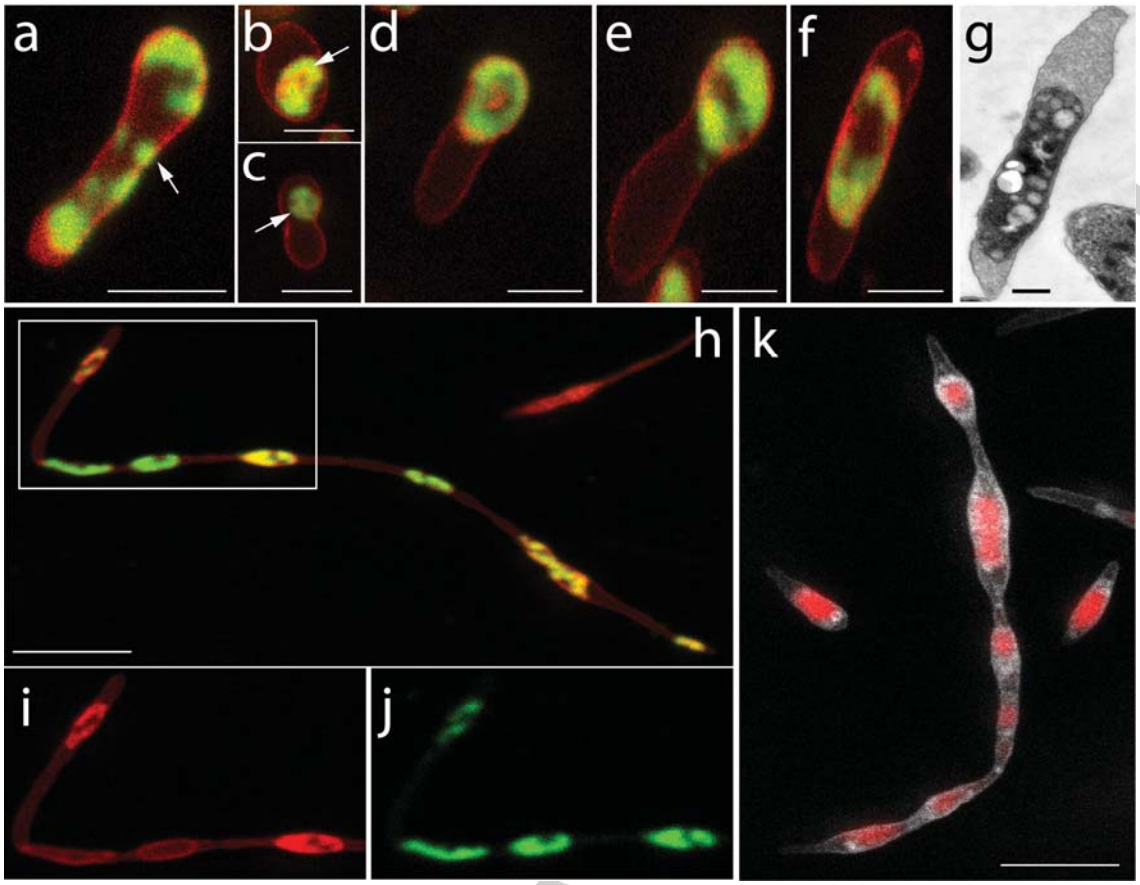

Figure 5. Membrane phase separation in *RS-P* cells during different growth stages. Images a-f and h-j show *RS-P* cells stained with universal membrane stain, FM™5-95 (red), and membrane stain that specifically stains L_d-membrane, *FAST*™ Dil (green). Arrow in images-a point to regions of the cell with L_d-membrane (also shown in Figure S5). Images b & c show later growth stage cells with arrows pointing to the cytoplasmic compartment, exclusively enclosed in L_d-membrane. Images e-f show subsequent growth stage *RS-P* cells with L_d-membrane restricted to poles. Image-g shows a TEM image of a similar *RS-P* cell with enlarged periplasmic space and intracellular membrane vesicles. A comparison of STED and TEM images of *RS-P* is presented in Figure S6. Image-h shows images of late log-phase filamentous *RS-P* cell. Images of this cell along its z-axis were shown in Figures S7 & S8. Images I & j show magnified regions of the filament in individual channels. Image-k shows filamentous *RS-P* cells stained with membrane and DNA dyes as mentioned in Figure 1. Scale bars: 1µm (a-f), g (500nm) and 10µm (g-i).

Also, in accordance with ADE theory[21], the morphological transformation of *RS-P* is associated with membrane phase-separation (Figure 5& S5-S8). The sequential steps of membrane phase-separation observed in *RS-P* are similar to what was proposed by the lipid-raft hypothesis[25]. During early growth stages, the cell membrane underwent phase-separation with liquid-disordered (L_d) regions forming small patches within the cell membrane (Figure 5a & S5a). Overtime, the inner membrane of the cell is exclusively composed of L_d and the outer membrane of the cell is exclusively composed of liquid-ordered (L_o)-membrane (Figure 5b-d). This enrichment of L_d-membrane around the cytoplasm could have been due to the constant loss of L_o-membrane in the form of hollow membrane buds into the periplasmic space (Figure S1). This budding of phase-separated membranes can be explained by the model proposed by Lipowsky & Jülicher[26,27]. In cells of subsequent growth stages, the presence of L_d-

membrane was restricted to the poles (Figure 5e & 5f), where the membrane experiences a high spontaneous curvature and the central barrel connecting the poles was noticed to be composed of L_o-membrane (Figure 5e & 5f). Given the L_d and L_o-membranes are largely composed of unsaturated and saturated phospholipids respectively, we presume lipid molecules in the membrane underwent self-organization with unsaturated phospholipid rich L_d-membrane translocating to regions of the cells with high spontaneous curvature (the cell poles) and distribution of L_o-membrane being restricted to linear regions of the cell membrane, where membrane experiences a low curvature. Similarly, localization of L_d and L_o-membranes selectively in the inner and outer membrane of the cell could also be explained by a combination of physical properties of cytoplasm and organizational principles leading towards a stable and lowest free energy state. Given the constant movement of the cytoplasmic compartment of the cell (Movie S1 & S2), it could have been energetically favorable to encapsulate cytoplasm with a more fluid L_d-membrane rather than more rigid L_o-membrane. Lipid raft hypothesis[25] and the existence of phase-separated membrane in live cells has been a point of contention among researchers[28], to date such membrane phase-separation and its physiological significance have only been reported in LVs[29]. To the best of our knowledge, ours is the first study to provide visual evidence of distinct phases in the cell membranes (Figure 5) and describe their evolutionary significance.

Earlier studies proposed that fission of protocells into daughter cells should have been achieved through physical forces[7,30]. Hence to achieve protocell fission, these studies employed methods like extrusion through a narrow pore size filter or by application of external force[7,30,31]. As most of the cells in the last growth stage are primarily unicellular daughter cells that were formed by the fission of filamentous *RS-P* and given the fact that our experiments were conducted under static conditions, we do not assume the fission of cells was a result of an external stimulus. We rather propose that fission of daughter cells was achieved by forces internal to the cell and was either a result of internal metabolic reactions[32] or constant movement of intracellular constituents[33]. It was also hypothesized that the presence of internal metabolism could lead to shape instabilities on the cell surface ultimately leading to cell division[32]. In support of this presumption, filamentous cells in our incubations were intrinsically unstable (Movie S3-S4). A constant pull-push motion of individual cells within the filament was often observed in *RS-P* (Movie S3-S5). This constant movement should have been caused by the Brownian movement of intracellular constituents[33,34] (Movie S1 & movement of DNA in spherical *RS-P* cells in the top half of the Movie S2). This constant movement of intracellular constituents could have led to the generation of force required for the fission of daughter cells.

WILEY-VCH

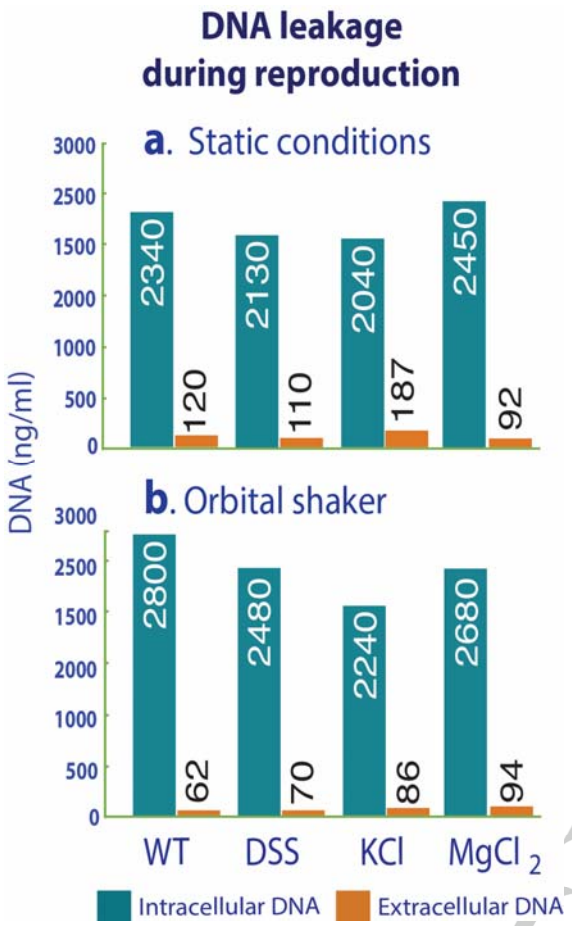

Figure 6. Quantification of DNA leakage, as an indication of *RS-P's* reproductive efficiency. Images a & b show a comparison of the amount (n=5) of extracellular and intracellular DNA (ng/ml) when *RS-P* was grown under static conditions (a) and while shaking (b). Annotations, WT (wild type, *R. sphaeroides* with a cell wall grown in NB); DSS, KCl & $MgCl_2$ – *RS-P* grown in NB with respective salts.

Another factor that could have contributed to constant deformations on the cell surface which ultimately led to the fission could have been the asymmetric conditions on either side of the cell membrane – organic carbon within the cell and inorganic salts outside the cell. Together with the movement of intracellular constituents, such conditions are known to induce constant deformation on the membrane surface[35]. In support of this presumption, the addition of bactericidal compounds like sodium azide (0.3%)[36] or formaldehyde/gluteraldehyde[37] did not have any influence on the surface deformations of the cells. These constant surface deformations could only be halted when conditions inside and outside the cells were equilibrated by creating pores within the membrane using detergents like Triton X-100 (0.5%), suggesting that asymmetric conditions on either side of the cell membrane contributed to the deformation of cells and provided the force required to mediate cell fission. Based on the above inferences we argue that the fission of parent cells into daughter cells was mediated by physiochemical forces generated by internal metabolism[32], random movement of cytoplasmic constituents (movement of intracellular DNA in Movie S2), deformations caused by transient binding of cations to the membrane surface[38] and asymmetric environmental conditions on either side of the cell membrane in terms of osmolarity or nature of the solute[35]. All these conditions are shown to generate shape instabilities, which could have led to the fission of cells[32] (Movies S3-S5). Nevertheless, the relative

contribution of each of these processes to the fission of parent cells is hard to determine in live cells, especially given their metabolic and compositional complexity.

To simulate Archaean Eon Ocean salinities, we grew *RS-P* in 5-10% DSS-NB in all the above experiments. DSS is a mixture of several mono and divalent salts like NaCl (38%wt), KCl (9%wt), $MgCl_2$ (42%wt), and other inorganic salts. These cations are known to interact differently with phospholipid membranes and are known to alter their physical properties[12,35]. Hence, in the subsequent experiments, we attempted to understand the influence of individual salts on the morphology of *RS-P*. To test this, we repeated the above experiments replacing DSS with an equivalent concentration of divalent and monovalent salts like $MgCl_2$ or KCl/NaCl. When grown in the presence of monovalent salts (7%KCl-NB), *RS-P* exhibited morphologies and reproduced by processes very similar to the ones observed when grown with DSS (Figure S9); except for forming thicker and longer filamentous cells with larger lenticular structures Similar cell morphologies were also observed when *RS-P* was grown in $MgCl_2$, with the exception that cell sizes were considerably smaller (Figure S10). Most cells observed in these incubations were of thin filamentous morphology. Thick tubular cells or lenticular cells with diameters >1-2µm were rarely observed (sometimes only transiently during the mid-growth stages) (Figure S10c, d & e). Unlike when grown in DSS or KCl, cells in their last growth stage were mostly uniform in their morphology (Figure S10i). Cells of this stage are predominantly unicellular daughter cells or cells in dyad undergoing binary fission.

Different morphologies exhibited by *RS-P* when grown in the KCl and $MgCl_2$ could be due to the nature of the interaction between phospholipid membranes and different cations[12]. It was reported that divalent cations like Mg^{+2} organize lipids into clusters of 10-15 molecules each[39]. This in turn dehydrates and increases the stiffness of the membrane making its area expansion energetically unfavorable. On the other hand, monovalent cations like K^+ are known to reduce the bending rigidity of the membrane, making the membrane more flexible[35]. This phenomenon could explain the easy expansion of the cell membrane, conducive to the formation of larger cells in the presence of KCl and smaller cell sizes when grown in the presence of $MgCl_2$.

Cells in all the experiments above were grown under static conditions. Given such conditions are rarely encountered in natural environments, we repeated the above experiments under multiaxial elongational flow conditions by growing *RS-P* on an orbital shaker. Under these growth conditions, cells exhibited a more uniform morphology irrespective of the nature of the salt (Figure S11). Little morphological variation was observed during different growth stages. Most cells during lag, log, and stationary growth stages were either individual cells or cells in dyad undergoing binary fission. Other cell morphologies were rarely observed. When *RS-P* was transferred between growth media containing different salt compositions or grown under static or stirring conditions, morphologies of *RS-P* changed reversibly. This reversible change suggests that the morphology of *RS-P* is determined by environmental conditions rather than the information encoded in its genome.

WILEY-VCH

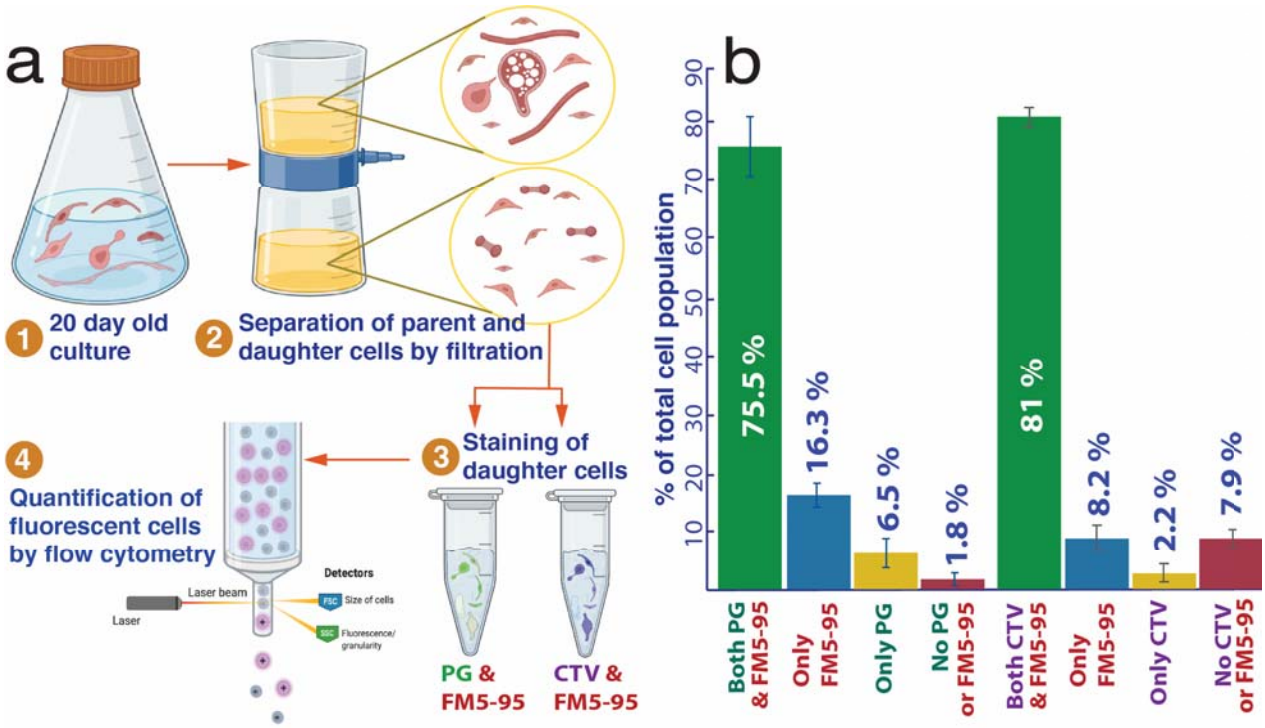

***Figure 7*. Presence of DNA and cytoplasmic activity in *RS-P* daughter cells.** Panel-a shows the workflow of the experiment. Image-b shows the percentage of *RS-P* daughter cells that received DNA from the parent cell and possess cytoplasmic activity as determined by staining the cells with dyes specific for cell membrane (FM™5-95), DNA (PicoGreen™ - PG), and cytoplasmic activity (CellTrace™ Violet - CTV). The relative percentages of cells stained with individual, and combinations of these dyes were quantified by flow cytometry. The original flow cytometry plots together with the confocal microscope images of daughter cells were shown in Figure S12 & S13.

The reproductive efficiency of *RS-P* is determined by quantifying the leakage of cell constituents during *RS-P*'s lifecycle[7]. Comparison of DNA concentrations within and out of the cell during the late log phase (Figure 6g & 6h), suggests that *RS-P* reproduced with similar efficiency as cells in their native form with functioning molecular biological mechanisms. Given the considerable amount of membrane debris (Figure S14) observed during the stationary growth phase, we propose that *RS-P* reproduced rather inefficiently. Nevertheless, reproductive efficiency was dependent on environmental conditions (Figure 6). Relatively less wastage of cell constituents and production of membrane debris was observed when *RS-P* was grown in the presence of $MgCl_2$ (Figure S10) than when cultured in DSS or KCl. Reproductive efficiency was also higher when *RS-P* was cultured under non-static conditions (Figure 6). Despite the wastefulness of its reproduction process under some environmental conditions, all our incubations resulted in viable daughter cells with cytoplasmic activity and intracellular DNA (Figure 7). Subsequent transfer of these cells either directly or after passing through 0.44µm filter (Figure 7) to separate the small daughter cells from other large cells and membrane debris into fresh media always resulted in growth. This mechanism of reproduction and the efficiency of the process is comparable to theoretical propositions of protocell reproduction[7], proposed from studying LVs.

WILEY

Conclusion: Our work alters the current presumption that molecular biological processes are necessary for mediating complex biological processes like cell replication. Our observations suggest that reproduction is an innate physicochemical property of cells with internal metabolism. In the absence of molecular biological processes, cell reproduction is governed entirely by the physiochemical properties of the cell constituents. Nevertheless, the efficiency of the process is considerably lower in the absence of molecular biological mechanisms. Given the simplicity and efficiency with which cells reproduced under environmental conditions of early Earth, we propose that primitive protocells inhabiting early Earth could have reproduced in a similar way. In our subsequent work, we were able to demonstrate from the fossil record that cells reproducing by the above described processes in-deed existed on early Earth[40].

Author contributions: DK conceived the work with input from TL, BZ, ML & JHK. DK performed laboratory experiments. AK did TEM imaging. DK & ML performed confocal super-resolution light microscopy imaging. DK & JHK wrote the manuscript with input from TL, BZ, ML, & AK.

Acknowledgments: We would like to thank Petra Schwille for her support and scientific input throughout the work and in preparing the manuscript. We would like to thank Gabriella Berthal and Markus Oster for excellent technical support. We would also like to thank Advanced Light Microscopy Facility at EMBL, Heidelberg, Ulf Schwartz from Leica Microsystems, colleagues at Ecological microbiology (Bayreuth University) and Cellular and Molecular Biophysics laboratory (Max Planck institute for Biochemistry) for their support throughout the work. This research was funded by the European Research Council (ERC), grant agreement 616644 (POLLOX) to TL, DFG-TRR174 to PS and Origins Excellence Cluster seed money to DK.

Keywords: Protocells, Gram-negative protocells, protocell replication, Cell-division, Early life.

(1) Oparin, A. I. *R. Inst. Chem. Rev.* **1969**, *2*, 1-12.
(2) Miller, S. L. *Science.* **1953**, *117*, 528–529.
(3) Mariani, A.; Russell, D. A.; Javelle, T.; Sutherland, J. D. *J. Am. Chem. Soc.* **2018**, *140*, 8657-8661.
(4) Powner, M. W.; Gerland, B.; Sutherland, J. D. *Nature* **2009**, *459*, 239-242.
(5) Rajamani, S.; Ichida, J. K.; Antal, T.; Treco, D. A.; Leu, K.; Nowak, M. A.; Szostak, J. W.; Chen, I. A. *J. Am. Chem. Soc.* **2010**, *132*, 5880-5885.
(6) Chen, I. A.; Salehi-Ashtiani, K.; Szostak, J. W. *J. Am. Chem. Soc.* **2005**, *127*, 13213–13219.
(7) Zhu, T. F.; Szostak, J. W. *J. Am. Chem. Soc.* **2009**, *131*, 5705-5713.
(8) Budin, I.; Debnath, A.; Szostak, J. W. *J. Am. Chem. Soc.* **2012**, *134*, 20812-20819.
(9) Wu, L. J.; Lee, S.; Park, S.; Eland, L. E.; Wipat, A.; Holden, S.; Errington, J. *Nat. Commun.* **2020**, *11*, *4149*.
(10) Leaver, M.; Dominguez-Cuevas, P.; Coxhead, J. M.; Daniel, R. A.; Errington, J. *Nature* **2009**, *457*, 849-853.
(11) Briers, Y.; Walde, P.; Schuppler, M.; Loessner, M. J. *Bioessays* **2012**, *34*, 1078–1084.
(12) Tsai, H. H. G.; Lai, W. X.; Lin, H. Da; Lee, J. Bin; Juang, W. F.; Tseng, W. H. *Biochim. Biophys. Acta - Biomembr.* **2012**, 1818, 2742-2755.
(13) Blake, R. E.; Chang, S. J.; Lepland, A. *Nature* **2010**, *464*, 1029–1032.
(14) Catling, D. C.; Zahnle, K. J. *Sci. Adv.* **2020**, *6*, eaax1420.
(15) Knauth, L. P. *Nature* **1998**, *395*, 554.

WILEY-VCH

(16) Moore, E. K.; Jelen, B. I.; Giovannelli, D.; Raanan, H.; Falkowski, P. G. *Nature Geoscience*. 2017, *10*, 629-636.
(17) Johnson, T. E.; Brown, M.; Kaus, B. J. P.; Vantongeren, J. A. *Nat. Geosci.* **2014**, *7*, 47-52.
(18) Mercier, R.; Kawai, Y.; Errington, J. *Cell.* **2013**, *152* (5), 997–1007.
(19) Narsimhan, V.; Spann, A. P.; Shaqfeh, E. S. G. *J. Fluid Mech.* **2015**, *777*, 1–26.
(20) Yanagisawa, M.; Imai, M.; Taniguchi, T. *Phys. Rev. E - Stat. Nonlinear, Soft Matter Phys.* **2010**, *82*, 051928-1-9.
(21) Yanagisawa, M.; Imai, M.; Taniguchi, T. *Phys. Rev. Lett.* **2008**, *100*, 148102-4.
(22) Kantsler, V.; Segre, E.; Steinberg, V. *Phys. Rev. Lett.* **2008**. *101*, 048101- 4.
(23) Sanborn, J.; Ogl□cka, K.; Kraut, R. S.; Parikh, A. N. *Faraday Discuss.* **2013**, *161*, 167-176.
(24) Bobrovska, N.; Góźdź, W.; Kralj-Iglič, V.; Iglič, A. *PLoS One* **2013**. *8*, 0073941.
(25) Simons, K.; Ikonen, E. **1997**. *387*, 569-572.
(26) Lipowsky, R. *J. Phys. II* **1992**, *2*, 1825-1840.
(27) Jülicher, F.; Lipowsky, R. *Phys. Rev. Lett.* **1993**, *70*, 2964.
(28) Sezgin, E.; Levental, I.; Mayor, S.; Eggeling, C. *Nature Reviews Molecular Cell Biology* **2017**, *18*, 361-374.
(29) Dreher, Y.; Jahnke, K.; Bobkova, E.; Spatz, J. P.; Göpfrich, K. *Angew. Chemie - Int. Ed.* **2021**, *60* 10661-10669.
(30) Deshpande, S.; Spoelstra, W. K.; Van Doorn, M.; Kerssemakers, J.; Dekker, C. *ACS Nano* **2018**, *12*, 2560–2568.
(31) Hanczyc, M. M.; Fujikawa, S. M.; Szostak, J. W. *Science.* **2003**, *302*, 618–622.
(32) Zwicker, D.; Seyboldt, R.; Weber, C. A.; Hyman, A. A.; Jülicher, F. *Nat. Phys.* **2017**, *13*, 408-413.
(33) Di Rienzo, C.; Piazza, V.; Gratton, E.; Beltram, F.; Cardarelli, F. *Nat. Commun.* **2014**, *5*, 5891.
(34) Fisher, J. K.; Bourniquel, A.; Witz, G.; Weiner, B.; Prentiss, M.; Kleckner, N. *Cell* **2013**, *153*, 882-885.
(35) Karimi, M.; Steinkühler, J.; Roy, D.; Dasgupta, R.; Lipowsky, R.; Dimova, R. *Nano Lett.* **2018**, *18*, 7816-7821.
(36) Levy, S.; Chevion, M. *Environ. Toxicol. Chem.* **2009**, *28*, 1380-1389.
(37) Spahn, C.; Grimm, J. B.; Lavis, L. D.; Lampe, M.; Heilemann, M. *Nano Lett.* **2019**, *19*, 500-505.
(38) Tarun, O. B.; Okur, H. I.; Rangamani, P.; Roke, S. *Commun. Chem.* **2020**, 3, article number 17.
(39) Schultz, Z. D.; Pazos, I. M.; McNeil-Watson, F. K.; Lewis, E. N.; Levin, I. W. *J. Phys. Chem. B* **2009**. *113*, 9932-9941.
(40) Kanaparthi, D.; Lampe, M.; Zhu, B.; Boesen, T.; Klingl, A.; Schwille, P.; Lueders, T. *bioRxiv* **2021**, 2021.08.16.456462.

WILEY-VCH

Entry for the Table of Contents

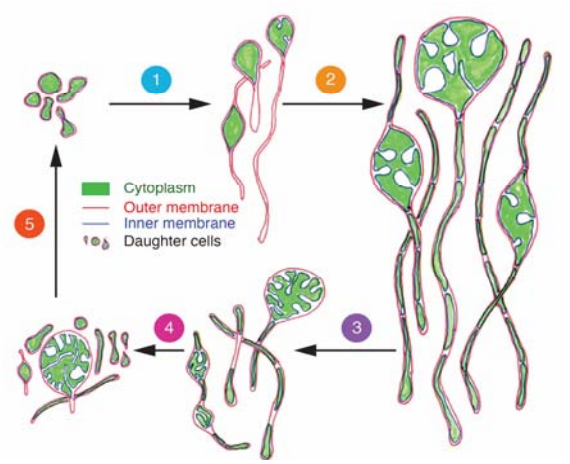

Here we present the simplest of all cell replication processes. This process does not require any guidance from the canonical molecular biological processes and is mediated entirely by the physicochemical properties of cell constituents and the chemical composition of the environment. Given the consistency and simplicity, we propose protocells reproduced by a similar process.

WILEY-VCH

WILEY-VCH